Available online at www.sciencedirect.com
ScienceDirect
Journal of Environmental Sciences 2011, 23(7) 1205–1210
JOURNAL OF ENVIRONMENTAL SCIENCES
ISSN 1001-0742
CN 11-2629/X
www.jesc.ac.cn

Preparation methods and thermal stability of Ba-Mn-Ce oxide catalyst for NO*x*-assisted soot oxidation

Xiaodong Wu*, Fan Lin, Lei Wang, Duan Weng, Zhou Zhou

Laboratory of Advanced Materials, Department of Materials Science and Engineering, Tsinghua University, Beijing 100084, China.
E-mail: wuxiaodong@tsinghua.edu.cn

Received 20 August 2010; revised 08 November 2010; accepted 15 November 2010

Abstract

Manganese oxide-loaded and -doped ceria as well as the corresponding barium-modified oxide catalysts were prepared for soot oxidation in the presence of NO*x*, and were characterized by using X-ray diffraction, Brunauer-Emmett-Teller and NO temperature-programmed oxidation measurements. The activity of catalyst depended strongly on the NO_2 production capacity, and the importance of surface nitrates was weakened without heat transfer limitations. The formation of perovskite-type oxides after the high-temperature calcination caused the loss of NO*x* storage capacity for the Ba-modified catalysts, but did not seem to affect the NO oxidation activity obviously. The addition of barium did not prevent the phase separation of MnO*x*-CeO_2 solid solutions, whereas it inhibited the sintering of oxide crystallites effectively. This, as well as the relatively high surface area, resulted in a small increase in soot oxidation temperature for the thermally aged Ba/Mn-Ce catalyst.

Key words: manganese oxide; ceria; barium; soot oxidation; NO_2; ageing

DOI: 10.1016/S1001-0742(10)60533-5

Citation: Wu X D, Lin F, Wang L, Weng D, Zhou Z, 2011. Preparation methods and thermal stability of Ba-Mn-Ce oxide catalyst for NO*x*-assisted soot oxidation. Journal of Environmental Sciences, 23(7): 1205–1210

Introduction

Diesel particulate filter (DPF) is considered as the most efficient method for achieving low soot emission from diesel engines, however, the filter regeneration remains as a technique challenge. Many catalysts have been proposed for filters performing both filtration and catalytic combustion of soot. Platinum-based catalysts seem to represent the best solution up to date, providing NO oxidation to NO_2 which allows soot oxidation at quite low temperatures (Jeguirim et al., 2007; Kalogirou et al., 2007).

However, the soot oxidation rate is limited by low NO*x* concentrations in exhaust gas from modern engines. The NO*x* storage feature of alkali metals, such as potassium, can provide additional desorbed NO*x* at moderate temperatures which makes them promising components in soot oxidation catalysts (Peralta et al., 2009; Gross et al., 2009; Sánchez et al., 2009; Weng et al., 2008). Despite the high activity, a drawback of potassium-containing catalysts emerges with low stability which comes along with the low melting point and solubility of K (Badini et al., 1996; Aneggi et al., 2008). Recently, barium supported oxide catalysts have received much attention, including Ba-K/CeO_2 (Peralta et al., 2006; Milt et al., 2007), Co-Ba-K/CeO_2 (Milt et al., 2003), Co-Ba-K/ZrO_2 (Milt et al., 2008; Banús et al., 2009, 2010) and Co-Ba-K/Al_2O_3 (Sui and Yu, 2008). However, only a few reports are involved with K-free barium catalysts (Castoldi et al., 2009; Kustov and Makkee, 2009; Wu et al., 2010a).

It is found in our previous work (Wu et al., 2010b) that, under an energy transference controlled regime, the impregnation of barium on MnO*x*-CeO_2 mixed oxides can effectively lower the soot oxidation temperature in the presence of NO*x* via a so-called "trigging" effect of the nitrate/nitrate-derived NO_2. However, the catalytic behavior without heat transfer limitations and thermal stability of this ternary catalyst have not been investigated. In this work, manganese-loaded and -doped ceria as well as the corresponding barium-modified catalysts were prepared by different methods to achieve high soot oxidation activity in the presence of NO. The thermal stability of the catalyst was also evaluated by treating in air at 800°C for 10 hr. The roles of manganese and barium in NO*x*-assisted soot oxidation were discussed.

1 Materials and methods

1.1 Catalyst preparation

MnO*x*-CeO_2 mixed oxides (Mn-Ce) were prepared by a sol-gel method. The nitrates $Ce(NO_3)_3{\cdot}6H_2O$ (99.0 wt.%,

* Corresponding author. E-mail: wuxiaodong@tsinghua.edu.cn

Beijing Yili Co., China) and $Mn(Ac)_2{\cdot}4H_2O$ (99.0 wt.%, Sinopharm Chemical Reagent Beijing Co., China) were mixed in deionized water according to the molar ratio of Mn:Ce 15:85. The citric acid was added as the complexing agent with a 1.5:1 ratio of the acid to metal ions including Ce^{3+} and Mn^{2+}. Polyglycol was followed with the weight of 10% citric acid addition. The solution was sufficiently stirred and heated at 80°C, till a gel was formed. The gel was dried at 110°C overnight followed by decomposition at 300°C for 1 hr and calcination at 500°C for 3 hr. The monoxide CeO_2 was prepared by a similar method.

The $Ba(Ac)_2$ (99%, Xilong Chemical, China) and $Mn(Ac)_2$ were co-impregnated on the home-made ceria following the ratio of $BaO/(BaO+Mn_2O_3+CeO_2)$ = 10 wt.%. The mixture was dried at 110°C for 2 hr and calcined at 550°C for 1 hr to obtain the Ba, Mn/Ce sample. The monometallic supported catalysts $MnOx/CeO_2$ (Mn/Ce) and $Ba/MnOx\text{-}CeO_2$ (Ba/Mn-Ce) with the given Mn and Ba contents were prepared by a similar method. The as-received samples were treated in muffle at 800°C for 10 hr to obtain the aged series.

1.2 Catalyst characterization

The powder X-ray diffraction (XRD) patterns were determined using a Japan Science D/max-RB diffractometer employing Cu $K\alpha$ radiation (λ = 0.15418 nm). The X-ray powder diffractograms were recorded at 0.02° intervals in the range of $20° \leqslant 2\theta \leqslant 80°$ with a scanning velocity of 4/min. The lattice constants and crystallite sizes of ceria in the samples were calculated based on Cohen's method and the Williamson-Hall equation, respectively.

The specific surface areas of the samples were measured using the N_2 adsorption isotherm at –196°C by the four-point Brunauer-Emmett-Teller (BET) method using an automatic surface analyzer (F-Sorb 3400, Gold APP Instrument, China). The samples were degassed at 200°C for 2 hr prior to the measurements.

The NO temperature-programmed oxidation (TPO) tests were carried out in a fixed-bed reactor with the effluent gases monitored by an infrared spectrometer (Thermo Nicolet iS 10, USA). The gas mixture of 1000 ppm NO/10% O_2/N_2 was fed to 100 mg of the sample (diluted with 300 mg of silica pellets) at a flow rate of 500 mL/min. The reactor temperature was ramped to 600°C at a heating rate of 10°C/min.

1.3 Activity measurement

Printex-U (Degussa, Germany) was used as a model soot. The soot and catalyst powders were mixed according to a weight ratio of 1:10 by a spatula for 2 min for "loose contact" conditions. The soot-catalyst mixture 110 mg was diluted with 300 mg of silica pellets to prevent reaction runaway. The TPO test was carried out from room temperature to 650°C at a heating rate of 10°C/min. The inlet gas mixture contained 1000 ppm NO, 10% O_2 with N_2 balance at a total flow rate of 500 mL/min. The outlet CO_2, CO, NO and NO_2 concentrations were determined by Nicolet iS 10. The light-off temperature (T_{50}) represented the temperature at which 50% of soot was oxidized to COx. The downstream CO_2/COx ratio during the whole soot oxidation was defined as the selectivity to CO_2 (S_{CO_2}).

2 Results and discussion

2.1 Solid properties

The powder XRD patterns of the fresh and aged samples are shown in Fig. 1a, b, respectively. Typical diffraction peaks of cubic ceria are observed for all the samples. For the fresh samples, barium mainly exists in the form of orthorhombic carbonate on the monometallic supported catalyst Ba/Mn-Ce, while it reacts with the co-impregnated manganese species to form the hexagonal perovskite oxides $BaMnO_3$ on Ba,Mn/Ce. Tetragonal Mn_3O_4 is formed on the loaded samples Mn/Ce and Ba,Mn/Ce. No manganese oxide phases are detected on the doped samples Mn-Ce and Ba/Mn-Ce, implying that Mn species may be in the form of highly dispersed oxide clusters (Sato and Komanoya, 2009) or may be partially incorporated into the ceria lattice.

After ageing, barium carbonate disappears on both the modified samples. The characteristic peaks of $BaMnO_3$ become sharpened on Ba,Mn/Ce, whereas typical peaks of orthorhombic $BaCeO_3$ are detected on Ba/Mn-Ce in

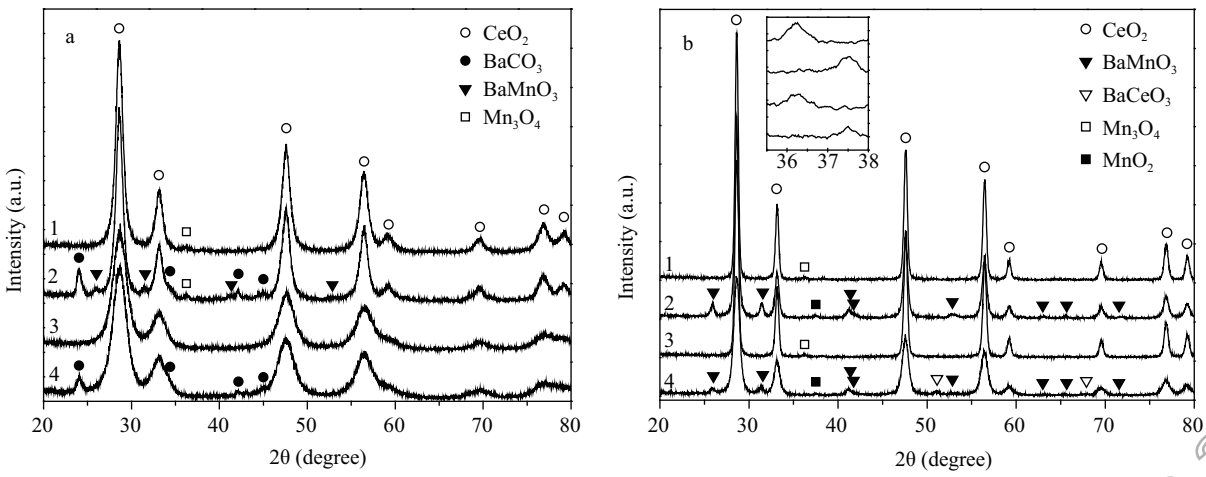

Fig. 1 XRD patterns of the fresh (a) and aged (b) samples. Line 1: Mn/Ce; line 2: Ba,Mn/Ce; line 3: Mn-Ce; line 4: Ba/Mn-Ce.

addition to those of $BaMnO_3$. That is, barium is preferable to reacting with manganese oxide on the former catalyst since they are co-impregnated on the surface of ceria, while it has more chance to react with ceria on the latter catalyst. Mn_3O_4 is detected on Mn-Ce due to the phase separation of the mixed oxides. It is interesting to find that the Mn species tend to exist in the form of tetragonal MnO_2 in the presence of barium. The sintering of MnO*x* clusters is less obvious on Mn-Ce based samples as indicated by the inner figure in Fig. 1b.

The structural parameters of the samples are listed in Table 1. The supported manganese or barium does not seem to enter into the ceria lattice or interact with ceria since the lattice constants of ceria in Mn/Ce and Ba, Mn/Ce are similar to that in ceria (0.5411–0.5412 nm) (Murugan et al., 2005; Aneggi et al., 2006). The decrease of the ceria lattice constant in Mn-Ce is ascribed to the incorporation of Mn^{x+} cations into the ceria lattice due to their smaller ionic radii (Mn^{3+}: 0.065 nm; Mn^{2+}: 0.083 nm; Ce^{4+}: 0.097 nm; Ce^{3+}: 0.114 nm). After ageing, the segregation of Mn cations causes an expansion of the ceria lattice for Mn-Ce and Ba/Mn-Ce. In regard to this view, the thermal stability of MnO*x*-CeO_2 mixed oxides is poor, and the addition of barium fails in preventing the separation of the solid solutions.

The incorporation of manganese into the ceria lattice results in finer crystallite sizes of the fresh Mn-Ce and Ba/Mn-Ce. Meanwhile, the impregnation of barium effectively inhibits the sintering of the ceria-based oxides. As a result, the Ba-modified catalysts show larger surface areas than the unmodified ones after ageing, although their fresh samples exhibit a certain loss in surface area due to blocking of the support pores by barium salt.

2.2 NO-TPO

NO_2 production performance is critical to soot catalytic oxidation in the presence of NO. In order to examine the activity of the catalysts for NO oxidation, the NO-TPO tests were carried out. The outlet NO_2 and NO*x* (NO+NO_2) curves over the fresh and aged catalysts are shown in Fig. 2a, b, respectively. The NO oxidation activity was determined by the availability and reactivity of active sites. Manganese oxide is a stronger oxidative component than ceria, and the strong synergistic effect between these two oxides endows Mn-Ce with the highest NO_2 production capacity. The oxidation ability of the oxide catalysts is weakened by the surface coverage with barium. Thus, the total NO_2 production during the whole temperature interval follows the order of Mn-Ce (4.1 mmol NO_2/g cat.) > Mn/Ce (3.5 mmol NO_2/g cat.) > Ba/Mn-Ce (3.3 mmol NO_2/g cat.) > Ba,Mn/Ce (3.2 mmol NO_2/g cat.). Meanwhile, the maximal NO_2 production temperature shifts towards higher temperatures by 20–30°C owing to the weakened NO oxidation ability and enhanced NO*x* adsorption capacity at low temperatures by introduction of the alkaline earth metal. It is known from the evolution of NO*x* that an obvious NO*x* adsorption occurs around 300°C on the Ba,Mn/Ce and especially Ba/Mn-Ce catalysts. The desorption of NO*x* occurs at temperatures higher than 430°C in the absence of reductants. Thus, the slightly higher NO_2 level does not contradict the thermodynamically predicted values.

Table 1 Structural parameters and soot oxidation activities of the samples

Catalyst	Lattice constant of CeO_2 (nm)	Crystallite size of CeO_2 (nm)	S_{BET} (m^2/g)	T_{50} (°C)	S_{CO_2} (%)
Mn/Ce	0.5412 (0.5411)	8 (18)	43 (1)	414 (532)	99 (50)
Ba,Mn/Ce	0.5412 (0.5412)	9 (15)	27 (2)	415 (466)	92 (81)
Mn-Ce	0.5406 (0.5411)	5 (17)	62 (4)	400 (500)	99 (61)
Ba/Mn-Ce	0.5407 (0.5412)	5 (10)	25 (8)	405 (429)	94 (94)

Values in parenthesis represent the corresponding data of the thermally aged samples.

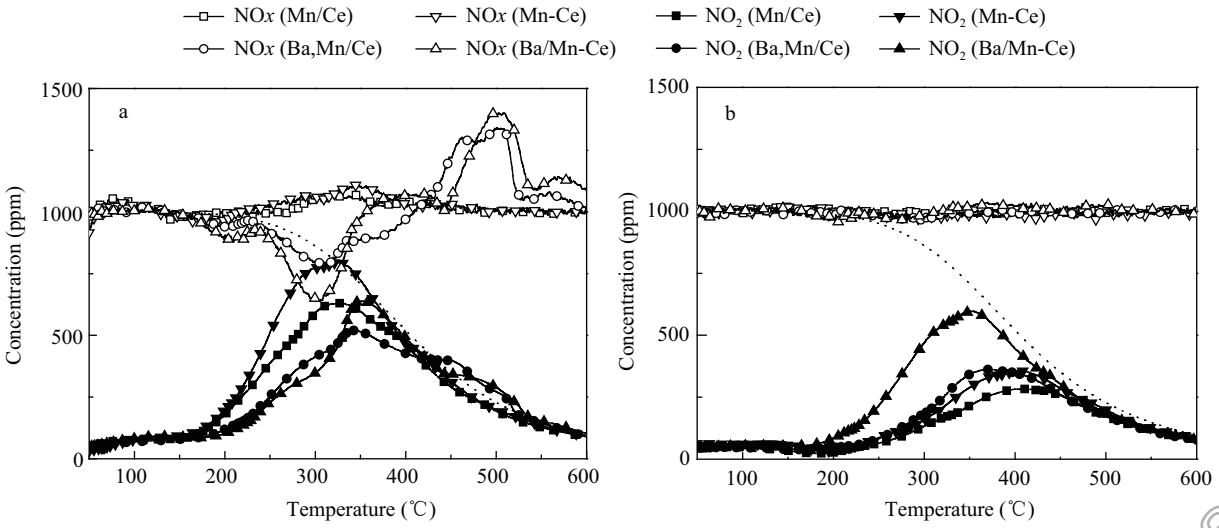

Fig. 2 NO-TPO profiles of the fresh (a) and aged (b) catalysts. The dotted line represents the NO_2 profile predicted by the thermodynamic equilibrium of the reaction NO + (1/2)O_2 ⟷ NO_2.

After ageing, the order of NO oxidation activity of the catalyst turns to be Ba/Mn-Ce (3.0 mmol NO_2/g cat.) > Ba,Mn/Ce (2.1 mmol NO_2/g cat.) > Mn-Ce (2.0 mmol NO_2/g cat.) > Mn/Ce (1.7 mmol NO_2/g cat.). Mn-Ce experiences a serious loss in NO oxidation activity due to the phase separation of the solid solutions, severe sintering of the oxide crystallites and reduction of the surface area. Its maximal NO_2 production temperature shifts from 326 to 402°C. On the other hand, the NO oxidation activity of Ba/Mn-Ce seems to be less affected, although its NO*x* storage capacity is almost completely lost mainly due to the formation of perovskites replacing barium carbonate. It has been shown that the addition of barium can effectively inhibit the sintering of oxides and keep manganese cations in a higher oxidation state during the high-temperature calcination, which facilitates to maintain high reactivity of active sites (Tang et al., 2010). It also implies that, in addition to manganese oxide (Tikhomirov et al., 2006), the perovskite-type mixed oxides may be also active for NO oxidation (Wen et al., 2007). Additionally, the relatively high surface area provides the aged Ba/Mn-Ce with abundant active sites.

2.3 Soot-TPO

The activities of the catalysts were evaluated by soot-TPO tests in the presence of NO, and the outlet CO*x* ($CO+CO_2$) and NO*x* curves of the fresh catalysts are shown in Fig. 3a and b, respectively. It has been widely reported that the bimodal shape of the CO*x* curves in Fig. 3a is caused by different dominant oxidizing agents at two stages. The low-temperature peak corresponds to the ignition of soot by NO_2, while the soot oxidation with O_2 is dominating at high temperatures (Wu et al., 2010c). Without the heat transfer limitations, the importance of NO_2 derived from decomposition of nitrates stored on the catalyst is significantly weakened, and that of NO_2 from oxidation of gaseous NO is highlighted. Thus, the contribution of barium as a NO*x* storage component to soot catalytic oxidation is limited. Meanwhile, the redox property of the Ba-modified catalyst is even reduced to some extent due to the surface covering with barium, resulting in a decreased reactivity of active oxygen with soot. Overall, the light-off temperatures of the fresh catalysts are similar to each other as listed in Table 1. The selectivity to CO_2 decreases slightly for the Ba-modified catalysts, which may arise from the predominance of reaction between the nitrates/nitrate-derived NO_2 and soot to produce CO which is further oxidized to CO_2 by O_2. In this sense, the NO rise occurring simultaneously with the onset of soot oxidation in Fig. 3b is thought to mainly arise from the decomposition of surface nitrates driven by the exothermic soot oxidation reaction. It is also supported by the fact that the NO*x* peaks appear at lower temperatures and are much intenser in respect to those in Fig. 2b.

Figure 4a and b shows the outlet CO*x* and NO*x* curves of the aged catalysts during soot-TPO tests, respectively. The light-off temperatures and selectivities to CO_2 are listed in Table 1. After ageing, the T_{50} for Ba/Mn-Ce catalyst shifts towards high temperatures by just 24°C, while the increase of T_{50} for Ba,Mn/Ce is about 50°C. The aged Ba-free catalysts experience a serious loss in activity with the shift of T_{50} by 100°C or even more, and their incomplete oxidation of soot become obvious. The NO*x* curve becomes almost flat for all the aged catalysts as shown in Fig. 4b, indicating a complete loss of NO*x* storage capacity. It can be seen that the soot oxidation activity of the aged catalysts follows a similar order of the NO_2 production capacity. Another important factor for the solid-solid-gas reaction is the surface area of the catalyst which determines the accessibility of the catalyst active sites (Wu et al., 2010d). That is, the relative high surface area and inhibited sintering of oxide crystallites result in high activities of the aged Ba/Mn-Ce for NO oxidation and hereby NO*x*-assisted soot oxidation.

3 Conclusions

Different preparation methods were compared to obtain high active and thermal stable Ba-Mn-Ce oxide catalysts for soot oxidation in the presence of NO. Without heat transfer limitations, the importance of nitrate-derived NO_2 is greatly weakened, and hereby the role of barium as a NO*x* storage component is not highlighted. The addition of barium does not prevent the phase separation of MnO*x*-CeO_2 solid solutions and itself form perovskite-type oxides during the high-temperature calcination. However, the

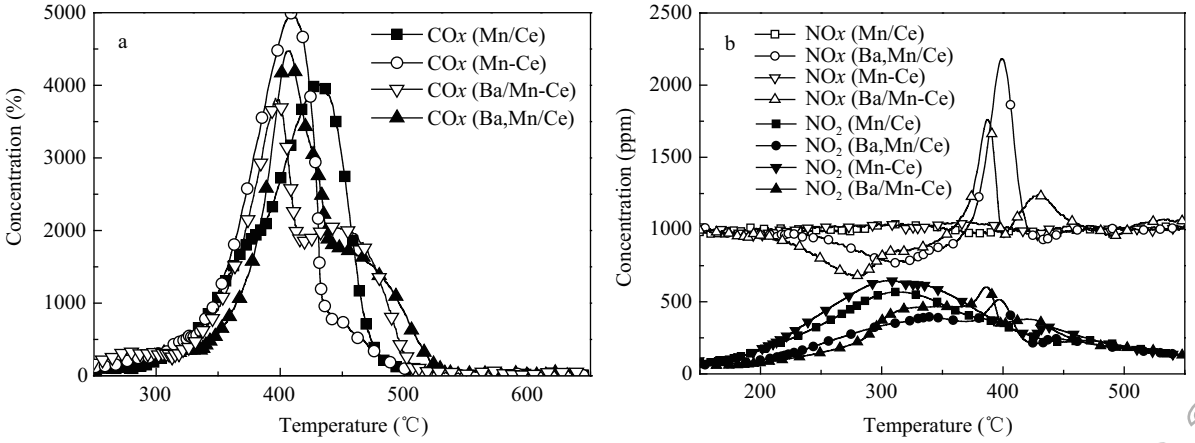

Fig. 3 Evolutions of CO*x* (a) and NO*x*/NO_2 (b) during soot-TPO tests with the fresh catalysts.

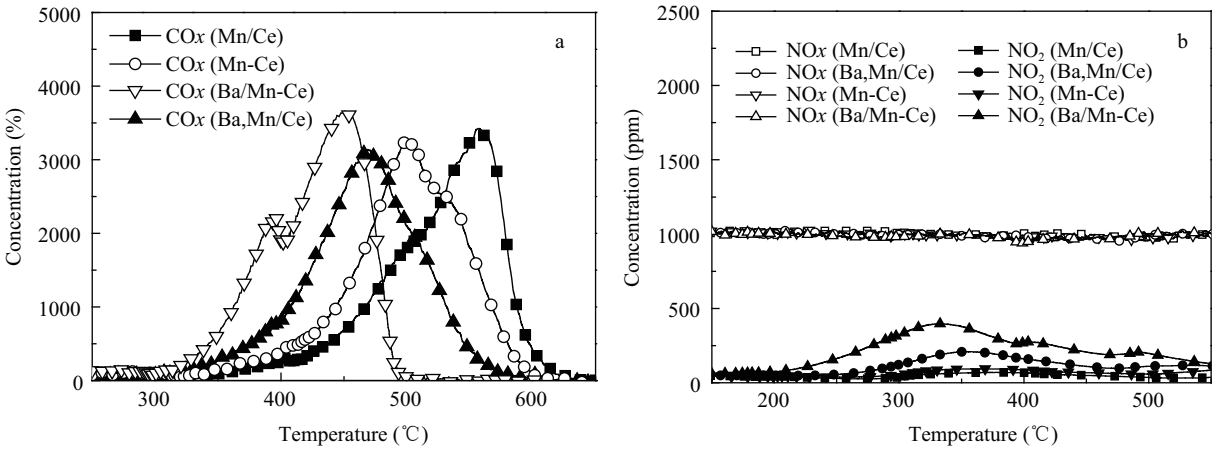

Fig. 4 Evolutions of CO*x* (a) and NO*x*/NO_2 (b) during soot-TPO tests with the aged catalysts.

sintering of oxide crystallites is effectively inhibited by the introduction of barium, which ensures the aged Ba/Mn-Ce catalyst a high activity for NO oxidation. This, as well as the relatively high surface area, results in a small shift of T_{50} for soot oxidation from 405 to 429°C after ageing.

Acknowledgments

This work was supported by the National Basic Research Program (973) of China (No. 2010CB732304) and the National Natural Science Foundation of China (No. 51072096).

References

Aneggi E, Leitenburg C, Dolcetti G, Trovarelli A, 2006. Promotional effect of rare earths and transition metals in the combustion of diesel soot over CeO_2 and CeO_2-ZrO_2. *Catalysis Today*, 114: 40–47.

Aneggi E, Leitenburg C, Dolcetti G, Trovarelli A, 2008. Diesel soot combustion activity of ceria promoted with alkali metals. *Catalysis Today*, 136: 3–10.

Badini C, Serra V, Saracco G, Montorsi M, 1996. Thermal stability of Cu-K-V catalyst for diesel soot combustion. *Catalysis Letters*, 37: 247–254.

Banús E D, Milt V G, Miró E E, Ulla M A, 2009. Structured catalyst for the catalytic combustion of soot: Co,Ba,K/ZrO_2 supported on Al_2O_3 foam. *Applied Catalysis A: General*, 362: 129–138.

Banús E D, Milt V G, Miró E E, Ulla M A, 2010. Co,Ba,K/ZrO_2 coated onto metallic foam (AISI 314) as a structured catalyst for soot combustion: Coating preparation and characterization. *Applied Catalysis A: General*, 379: 95–104.

Castoldi L, Matarrese R, Lietti L, Forzatti P, 2009. Intrinsic reactivity of alkaline and alkaline-earth metal oxide catalysts for oxidation of soot. *Applied Catalysis B: Environmental*, 90: 278–285.

Gross M S, Ulla M A, Querini C A, 2009. Catalytic oxidation of diesel soot: New characterization and kinetic evidence related to the reaction mechanism on K/CeO_2 catalyst. *Applied Catalysis A: General*, 360: 81–88.

Jeguirim M, Tschamber V, Ehrburger P, 2007. Catalytic effect of platinum on the kinetics of carbon oxidation by NO_2 and O_2. *Applied Catalysis B: Environmental*, 76: 235–240.

Kalogirou M, Katsaounis D, Koltsakis G, Samaras Z, 2007. Measurements of diesel soot oxidation kinetics in an isothermal flow reactor-catalytic effects using Pt based coatings. *Topics in Catalysis*, 42-43: 247–251.

Kustov A L, Makkee M, 2009. Application of NO*x* storage/release materials based on alkali-earth oxides supported on Al_2O_3 for high-temperature diesel soot oxidation. *Applied Catalysis B: Environmental*, 88: 263–271.

Milt V G, Peralta M A, Ulla M A, Miró E E, 2007. Soot oxidation on a catalytic NO*x* trap: Beneficial effect of the Ba-K interaction on the sulfated Ba,K/CeO_2 catalyst. *Catalysis Communications*, 8: 765–769.

Milt V G, Querini C A, Miró E E, Ulla M A, 2003. Abatement of diesel exhaust pollutants: NO*x* adsorption on Co,Ba,K/CeO_2 catalysts. *Journal of Catalysis*, 220: 424–432.

Milt V G, Banus E D, Ulla M A, Miro E E, 2008. Soot combustion and NO*x* adsorption on Co,Ba,K/ZrO_2. *Catalysis Today*, 133-135: 435–440.

Murugan B, Ramaswamy A V, Srinivas D, Gopinath C S, Ramaswamy V, 2005. Nature of manganese species in $Ce_{1-x}Mn_xO_{2-\delta}$ solid solutions synthesized by the solution combustion route. *Chemistry of Materials*, 17: 3983–3993.

Peralta M A, Gross M S, Sánchez B S, Querini C A, 2009. Catalytic combustion of diesel soot: Experimental design for laboratory testing. *Chemical Engineering Journal*, 152: 234–241.

Peralta M A, Milt V G, Cornaglia L M, Querini C A, 2006. Stability of Ba,K/CeO_2 catalyst during diesel soot combustion: Effect of temperature, water, and sulfur dioxide. *Journal of Catalysis*, 242: 118–130.

Sánchez B S, Querini C A, Miró E E, 2009. NO*x* adsorption and diesel soot combustion over La_2O_3 supported catalysts containing K, Rh and Pt. *Applied Catalysis A: General*, 366: 166–175.

Sato T, Komanoya T, 2009. Selective oxidation of alcohols with molecular oxygen catalyzed by Ru/MnO*x*/CeO_2 under mild conditions. *Catalysis Communications*, 10: 1095–1098.

Sui L N, Yu L Y, 2008. Diesel soot oxidation catalyzed by Co-Ba-K catalysts: Evaluation of the performance of the catalysts. *Chemical Engineering Journal*, 142: 327–330.

Tang X F, Li J H, Sun L, Hao J M, 2010. Origination of N_2O from NO reduction by NH_3 over β-MnO_2 and α-Mn_2O_3. *Applied Catalysis B: Environmental*, 99: 156–162.

Tikhomirov K, Kröcher O, Elsener M, Wokaun A, 2006. MnO*x*-CeO_2 mixed oxides for the low-temperature oxidation of diesel soot. *Applied Catalysis B: Environmental*, 64: 72–78.

Wen Y X, Zhang C B, He H, Yu Y B, Teraoka Y, 2007. Cat-

alytic oxidation of nitrogen monoxide over $La_{1-x}Ce_xCoO_3$ perovskites. *Catalysis Today*, 126: 400–405.

Weng D, Li J, Wu X D, Lin F, 2008. Promotional effect of potassium on soot oxidation activity and SO_2-poisoning resistance of Cu/CeO_2 catalyst. *Catalysis Communications*, 9: 1898–1901.

Wu X D, Zhou Z, Weng D, Lin F, 2010a. Role of stable nitrates stored on BaCoCe in soot catalytic oxidation. *Catalysis Communications*, 11: 749–752.

Wu X D, Liu S, Lin F, Weng D, 2010b. Nitrate storage behavior of $Ba/MnOx\text{-}CeO_2$ catalyst and its activity for soot oxidation with heat transfer limitations. *Journal of Hazardous Materials*, 181: 722–728.

Wu X D, Lin F, Xu H B, Weng D, 2010c. Effects of adsorbed and gaseous NO*x* species on catalytic oxidation of diesel soot with $MnOx\text{-}CeO_2$ mixed oxides. *Applied Catalysis B: Environmental*, 96: 101–109.

Wu X D, Liu S, Weng D, Lin F, 2010d. Textural-structural properties and soot oxidation activity of $MnOx\text{-}CeO_2$ mixed oxides. *Catalysis Communications*, 12(5): 345–348.